Biowaste-Derived Lagerstroemia speciosa Fruit Shell Ash (WELSA) as an Efficient Green Catalyst for One- Pot Synthesis of 2-Amino-4H-Benzochromenes

Ashwini Pawar
Department of Chemistry, Raje Ramrao Mahavidyalaya, Jath, Dist. Sangli, 416404, Maharashtra, India
Arvind Pawar
Department of Chemistry, Raje Ramrao Mahavidyalaya, Jath, Dist. Sangli, 416404, Maharashtra, India
Sandeep Patil
Department of Chemistry, Padmabhushan Dr. Vasantraodada Patil Mahavidyalaya, Tasgaon, Dist. Sangli, 416312, Maharashtra, India
Sanyuja S. Patil
Department of Chemistry, Padmabhushan Dr. Vasantraodada Patil Mahavidyalaya, Tasgaon, Dist. Sangli, 416312, Maharashtra, India
Pradeep Patil
patilpradeep197@gmail.com
Department of Chemistry, DKTE Society's, Textile and Engineering Institute, Ichalkaranji 416115, MS, India
Suresh Patil
Department of Chemistry, Raje Ramrao Mahavidyalaya, Jath, Dist. Sangli, 416404, Maharashtra, India

Research Article

Keywords: Lagerstroemia speciosa fruit shells ash, Waste-derived catalyst, 2-Amino-4H-benzochromenes, Sustainable synthesis, Green solvent

Posted Date: July 13th, 2026

DOI: https://doi.org/10.21203/rs.3.rs-10178891/v1

Additional Declarations: No competing interests reported.

Biowaste-Derived *Lagerstroemia speciosa* Fruit Shell Ash (WELSA) as an Efficient Green Catalyst for One-Pot Synthesis of 2-Amino-4*H*-Benzochromenes

Ashwini Pawar[a], Arvind Pawar[a], Sandeep Patil[b], Sanyuja S. Patil[b], Pradeep Patil[c*], Suresh Patil[a]

[a]Department of Chemistry, Raje Ramrao Mahavidyalaya, Jath, Dist. Sangli, 416404, Maharashtra, India
[b]Department of Chemistry, Padmabhushan Dr. Vasantraodada Patil Mahavidyalaya, Tasgaon, Dist. Sangli, 416312, Maharashtra, India

[c]Department of Chemistry, DKTE Society's, Textile and Engineering Institute, Ichalkaranji 416115, MS, India

*Corresponding author: Tel: +91 9527702738; E-mail: patilpradeep197@gmail.com

Abstract

The utilization of waste materials in sustainable organic transformations offers the dual benefits of cost reduction and environmental remediation. In the present work, we report the waste derived catalyst (WELSA) prepared from the fruit shell ash of the naturally occurring plant *Lagerstroemia speciosa* (Family: Lythraceae) for the construction of 2-amino-4H-benzochromene derivatives. The catalyst was characterized using various analytical techniques, including FT-IR, XRD, EDX, SEM, and TGA analyses to decode its chemical composition. EDX analysis revealed a high percentage of potassium, along with other trace elements. The characterization studies indicated the predominance of potassium species, which are proposed to play a crucial role in efficiently promoting the reaction. The synthesis was carried out using naphthols, diversely substituted aromatic aldehydes, and malononitrile under ambient reaction conditions. This environmentally benign protocol offers several benefits, including the use of a renewable waste-derived catalyst, short reaction times, high product yields, operational simplicity, and excellent catalyst recyclability, with sustained catalytic performance over five consecutive reaction cycles.

Keywords: *Lagerstroemia speciosa* fruit shells ash, Waste-derived catalyst, 2-Amino-4*H*- benzochromenes, Sustainable synthesis, Green solvent

1 Introduction:

Green chemistry plays a crucial role in addressing many environmental and scientific challenges through promoting more safer and sustainable chemical practices. One of its central goals is the formulation of chemical processes that minimizes the use of hazardous substances, toxic or an unstable organic solvent ultimately reduces the waste generation. The exploration of alternative reaction media, optimization of reaction parameters, and utilization of environmentally-friendly catalysts are some of the approaches for advancing chemical synthesis. In this context, much attention has been paid to the exploration of natural and biodegradable materials for synthetic organic transformations [1]. Recently, agro-food waste-based catalysts have been widely used in catalysis because of their large surface area, biodegradability, low toxicity, cost-effectiveness, and recyclability [2]. There are numerous examples driven by waste-derived materials including esterification, oxidation, polymer decomposition, hydrogen evolution, photodecomposition of dyes, and catalytic reduction of pollutants, etc. [3].

In addition, several researchers have successfully developed waste-derived catalysts as sustainable alternatives to traditional catalytic systems [4-7]. From the literature survey, *Lagerstroemia speciosa* (Family: Lythraceae) possesses a rich mineral composition along with essential vitamins. The relative mineral composition was reported to be 60.84 % K, 25.72 % Ca, 5.56 % P, 3.48 % S, 2.73 % Fe, 0.52 % Zn, 0.49 %

Rb, 0.42 % Cu, and 0.24 % other trace elements, indicating notably high potassium content [8]. *L. speciosa* fruit also shows various pharmacological properties including antibacterial, anticancer, antidiarrhoeal, analgesic and cytotoxicity [9]. The catalyst is prepared by the simple thermal treatment of dried *L. speciosa* fruit shells. The predominance of potassium species in WELSA is presumed to play a significant role in enhancing its catalytic activity, particularly in multicomponent reactions. Multicomponent reactions (MCRs) have attracted great attention, as they provide easy and rapid access to large libraries of heterocyclic molecules with diverse substitution patterns [10]. MCRs often reduce reaction times and provide higher chemical yields compared to multistep syntheses, thereby lowering energy consumption. Consequently, the development of new MCRs under green reaction conditions has marked a significant milestone in drug discovery, organic synthesis, and materials sciences.

Benzochromenes constitute an important structural unit found in natural products and compounds of current therapeutic interest. **Figure 1** represents some naturally occurring bioactive benzochromenes, such as tetrahydrocannabinol [**A**], urolithin [**B**], epicalyxin F [**C**], and tectol [**D**], which exhibit multiple sclerosis, anti-inflammatory, anticancer, and antiplasmodial activities [11]. Benzochromene scaffolds and their analogues have also been reported to possess antimicrobial [12], antioxidant [13-14], antitubercular [15], anti-HIV activity [16], antibacterial [17], antidepressant [18], antihelminthic [19]. Furthermore, they have been used against central nervous system disorder [20], Alzheimer's disease, amyotrophic lateral sclerosis, Parkinson's disease, Huntington's disease, and other neurodegenerative disorders [21]. Such a broad spectrum of biological and medicinal applications has motivated the scientific community to develop efficient synthetic methodologies for the construction of benzochromene derivatives.

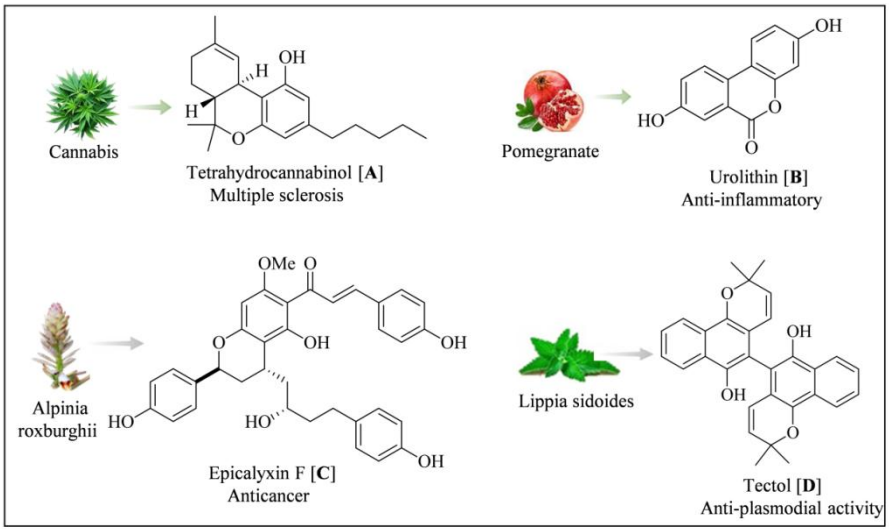

Fig. 1 Glimpse of plant products bearing benzochromene moieties.

In this regard, several methods have been reported for the synthesis of 4*H*-benzochromenes using homogeneous and heterogeneous catalysts such as triethylamine, 2-hydroxyethylammonium formate, Fe_3O_4@SiO_2@[O-$(CH_2)_2$-NH_2] [HCO_2H] [22], agave leaf ash extract [23]. Cu (II)salen complex grafted onto KCC-1 [24], sodium malonate [25] and wood ash biocatalysts [26]. Although these reported protocols possess certain advantages, many of them still suffer from several drawbacks, including the use of expensive catalytic precursors, high catalyst loading, toxic reagents, prolonged reaction times, and the generation of hazardous waste.

Therefore, there remains an urgent need to develop efficient, environmentally benign, and safer protocols under green reaction conditions. To the best of our knowledge, we herein report for the first time the use of a naturally sourced, mild, inexpensive, and non-toxic water extract of *L. speciosa* fruit shell ash as a waste-derived green catalyst (WELSA) for the one-pot three-component synthesis of 2-amino-4*H*-benzochromenes from naphthols, diversely substituted aldehydes, and malononitrile under ambient conditions (**Scheme 1**).

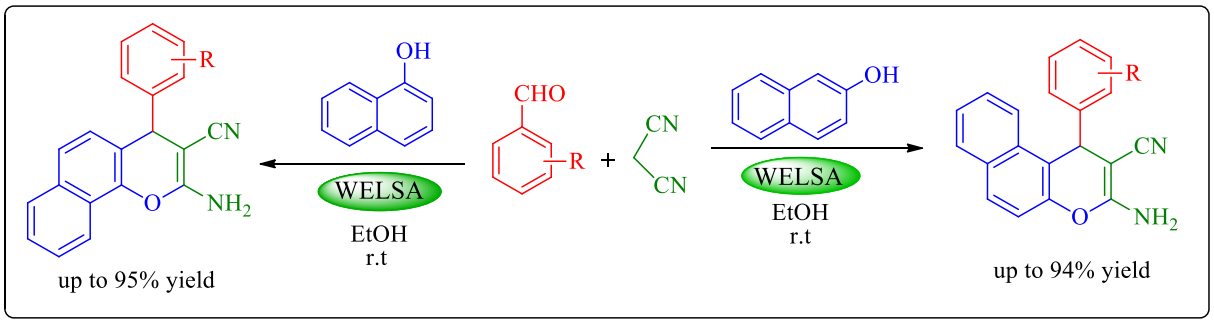

Scheme 1 Synthesis of 2-amino-4*H*-benzochromenes using WELSA catalyst.

2 Experimental

2.1 Materials and methods

The waste shells of the fruit *Lagerstroemia speciosa* were collected from the local area (Miraj, Dist. Sangli, MS, India) and authenticated in the Department of Botany, R.R. College, Jath (MS, India). All required chemicals were purchased from Sigma-Aldrich and used without further purification. The completion of the reactions and the purity of the products were monitored by TLC on Merck silica gel (60 F254) coated aluminum plates. The melting points were recorded using a DBK programmable melting point apparatus by the capillary method and are uncorrected. The FT-IR spectrum was recorded using a Bruker ALPHA FTIR spectrometer. Powder X-ray diffraction (XRD) analysis was carried out using a D2 Phaser diffractometer (Germany) operating with Cu Kα radiation (λ = 1.5406 Å) to assess the crystalline nature of the catalyst. Scanning electron microscopy (SEM) images were obtained using FEI NOVA Nano SEM 450 equipment. The elemental composition of the WELSA catalyst was determined using energy-dispersive X-ray (EDX) analysis on a Quanta 200 3D FEI instrument. ^{1}H and ^{13}C NMR spectra were recorded on an Avance 400 instrument using $CDCl_3$ and DMSO-d_6 as a dissolving solvent, with TMS as an internal standard. Chemical shifts (δ) are expressed in ppm.

2.2 Catalyst preparation

The waste fruit shells of *Lagerstroemia speciosa* were thoroughly washed using distilled water to remove the debris and dust particles. The cleaned fruit shells were dried using an oven at a temperature of 70 °C for 5 h. The dried shells were ground into a fine powder and further calcined in a muffle furnace at 700 °C at a heating rate of 2 °C/min for 2 h. The 10 g of soft ash obtained from this process was taken in distilled water (100 mL) and stirred at room temperature for 30 min. The suspension was then kept undisturbed at room temperature for 1 h to allow the ash particles to settle. Subsequently, the mixture was filtered using a Gooch crucible, and the collected filtrate (pH = 11) was stored at 4 °C. This filtrate was used as a catalyst for the synthesis of benzochromene derivatives. The stepwise preparation of the WELSA catalyst is illustrated in Figure 2.

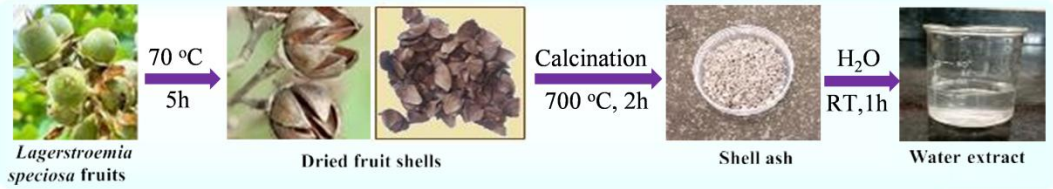

Fig. 2 Preparation of the WELSA catalyst

2.3 General procedure for the synthesis 2-amino-4*H*-benzochromenes (4a-r)

In a 25 mL round-bottom flask, a mixture of α-/β-naphthol (1 mmol), an aromatic aldehyde (1 mmol), malononitrile (1 mmol), aqueous extract of *Lagerstroemia speciosa* fruit shell ash (3 mL), and ethanol (3 mL) was stirred at room temperature for the time specified in Table 1. The progress of the reaction was monitored by TLC using ethyl acetate: n-hexane (2:3, v/v) as the mobile phase. Upon completion of the reaction, the precipitated product was filtered off. The crude product was then recrystallized from ethanol to obtain the pure product.

2.4 Spectral data of the synthesized compounds

2.4.1 2- Amino-4-(phenyl)-4*H*-benzo[*h*]chromene-3-carbonitrile (Table 2, entry 4a):

Pale Yellow; M.P. 204–206 °C (Lit. 205-207 °C) [32]; FT-IR (ATR) ν_{max}/cm^{-1}: 3344, 2851, 2223, 1605, 1571, 1445, 1278, 1153, 833, 609; ^{1}HNMR (DMSO-d_6, 400 MHz) δ (ppm): 4.80 (s, 1H), 7.01-7.27 (m, 8H), 7.46-7.48 (m, 3H), 7.78 (d, 2H), 8.24(d, 1H, Ar-H); ^{13}C NMR (DMSO-d_6, 100 MHz) δ (ppm): 160.38, 145.63, 143.30, 133.07, 128.00, 128.02, 127.68, 127.14, 124.07, 123.31, 121.26, 120.83, 117.71 57.34, 41.71; Elemental analysis; Calcd. (%) for $C_{20}H_{14}N_2O$: C, 80.50; H, 4.75; N, 9.35; found: C, 80.50; H, 4.70; N, 9.41.

2.4.2 2-amino-4-(4-nitrophenyl)-4*H*-benzo[*h*]chromene-3-carbonitrile (Table 2, entry 4b):

Dark Yellow; M.P. 236-240 °C (Lit. 238-239 °C) [32]; FT-IR (ATR) ν_{max}/cm^{-1}: 3371, 2223, 1605, 1512, 1319, 1184, 833, 610 cm $^{-1}$; ^{1}H NMR (DMSO-d_6, 400 MHz) δ (ppm): 5.03 (s, 1H), 7.00 (s, 2H), 7.46 (d, 1H), 7.50 - 7.56 (m, 5H, Ar-H), 7.78 (d, 2H, Ar-H), 8.07 (d, 1H, Ar-H); ^{13}C NMR (DMSO-d_6, 100 MHz) δ (ppm): 160.66,153.03, 146.88, 143.52, 133.32, 129.25, 127.82, 127.14, 124.01, 123.31, 121.34, 120.44, 114.47, 55.03; Elemental analysis: Calcd. (%) for $C_{20}H_{13}N_3O_3$: C, 69.97; H, 3.82; N, 12.24. Found: C, 69.93; H, 3.80; N, 12.21.

2.4.3 2-amino-4-(2,4-dichlorophenyl)-4*H*-benzo[*h*]chromene-3-carbonitrile (Table 2, entry 4c):

Light Yellow; M.P. 210-212 °C (Lit. 212-14 °C) [25]; FT-IR (ATR) ν_{max}/cm^{-1}: 3368, 2224, 1591, 1450, 1374, 1317, 1218, 1186, 957, 755 cm $^{-1}$; ^{1}H NMR (DMSO-d_6, 400 MHz) δ (ppm): 5.37 (s, 1H), 6.54 (d, 1H), 7.25 (d, 2H), 7.45- 7.50 (m, 4H, Ar-H), 8.25 (d, 1H, Ar-H); ^{13}C NMR (DMSO-d_6, 100 MHz) δ (ppm): 160.81, 143.52, 141.60, 133.29, 132.99, 129.30, 128.25, 127.80, 126.84, 125.54, 124.39, 123.22, 121,31, 120.35, 116.39, 55.29, 37.95; Elemental analysis: Calcd. (%) for $C_{20}H_{13}Cl_2N_2O$: C, 72.18; H, 3.94; N, 8.42. Found: C, 72.14; H, 3.91; N, 8.40.

2.4.4 2-amino-4-(4-hydroxyphenyl)-4*H*-benzo[*h*]chromene-3-carbonitrile (Table 2, entry 4d):

Off white; M.P. 242-246 °C (Lit. 244-45 °C) [25]; FT-IR (ATR) ν_{max}/cm^{-1}: 3028, 2851, 2223, 1605, 1571, 1440, 1370, 1319, 1278, 1185, 833, 808, 610 cm $^{-1}$; ^{1}H NMR (DMSO-d_6, 400 MHz) δ (ppm): 4.76 (s, 1H), 6.74 (s, 2H), 7.43-7.49 (m, 4H, Ar-H), 7.74 (m, 1H, Ar-H), 8.72-8.74 (d, 2H, Ar-H), 8.57 (s, 1H); ^{13}C NMR (DMSO-d_6, 100 MHz) δ (ppm): 160.04, 146.91, 145.88, 143.13, 136.69, 133.01, 127.61, 126.64, 126.47, 126.35, 123.89, 123.31, 121.20,120.88, 117.93, 112.97, 64.34, 58.3, 56.13, 41.19; MS: m/z: 314.10 (100.0 %); Found: 314; Elemental analysis: Calcd. (%) for $C_{20}H_{14}N_2O_2$: C, 76.42; H, 4.49; N, 8.91. Found: C, 76.39; H, 4.45; N, 8.90.

2.4.5 3-amino-1-(2,4-dichlorophenyl)-1H-benzo[f]chromene-2-carbonitrile (Table 2, entry 4g):

White solid; M.P. 238-240 °C (Lit. 240-42 °C) [25]; FT-IR (ATR) ν_{max}/cm^{-1}: 3033, 2227, 1584, 1555, 1490, 1409, 1291, 1256, 1008, 828, 616, 520 cm $^{-1}$; ^{1}H NMR (DMSO-d_6, 400 MHz) δ (ppm): 5.65 (s,1H), 6.77-6.88 (d, 2H), 7.08-7.10 (m, 4H, Ar-H), 7.25 (d, 2H, Ar-H), 7.25-7.42 (m, 4H, Ar-H), 7.83 (d, 1H, Ar-H), 8.01 (s, 1H); ^{13}C NMR, (DMSO-d_6, 100 MHz) δ (ppm): 160.27, 147.53, 141.85, 132.62, 132.35, 131.33, 131.12, 130.44, 130.04, 129.05, 128.8, 127.65, 125.24, 122.94, 120.10, 117.03, 114.65, 56.68, 34.93; Elemental analysis: Calcd. (%) for $C_{20}H_{13}Cl_2N_2O$: C, 72.18; H, 3.94; N, 8.42. Found: C, 72.15; H, 3.92; N, 8.40.

2.4.6 3-amino-1-(2-bromophenyl)-1H-benzo[f]chromene-2-carbonitrile (Table 2, entry 4h):

Pale Yellow; M.P. 244-246 °C (Lit. 246-248 °C) [25]; FT-IR (ATR) ν_{max}/cm^{-1}: 3033, 2227, 1583, 1555, 1489, 1291, 1095, 935, 828, 520 cm $^{-1}$; ^{1}H NMR (DMSO-d_6, 400 MHz) δ (ppm): 5.67 (s, 1H), 7.06 (s, 1H), 7.08 (s, 1H), 7.25-7.33 (m, 4H, Ar-H), 7.54 (d, 2H, Ar-H), 7.74-7.79 (m, 3H, Ar-H), 7.96 (d, 1H, Ar-H); ^{13}C NMR (DMSO-d_6, 100 MHz) δ (ppm): 160.21, 147.46, 144.75, 132.88, 131.14, 130.43, 130.36, 128.76, 128.67, 127.53, 125.19, 123.40, 122.25, 120.14, 117.07, 115.53, 57.29, 37.64; MS (m/z): 376 (100.0 %); Found: 377; Elemental analysis: Calcd. (%) for $C_{20}H_{13}ClN_2O$: C, 72.18; H, 3.94; N, 8.42. Found: C, 72.16; H, 3.93; N, 8.41.

3 Results and discussion

3.1 Characterization of Catalyst

FT-IR spectroscopy was employed to identify the key functional groups and surface characteristics of the WELSA catalyst, as shown in **Fig. 3**. The broad absorption bands at 3130 cm^{-1} and 2929 cm^{-1} correspond to C-H stretching vibrations, while the peak at 1649 cm^{-1} is attributed to O–H bending vibrations, indicating the presence of hydroxyl groups on the catalyst surface. A prominent band at 1407 cm^{-1} suggests the presence of metal carbonates. Another absorption band at 1119 cm^{-1} is assigned to Si-O linkage, whereas the peak at 874 cm^{-1} further confirms the presence of carbonate minerals in the catalyst matrix. Notably, the strong bands in the region of 619–420 cm^{-1} are characteristic of metal–oxygen (M-O) bonds, validating the formation of metal oxide species. Overall, the FTIR results confirm that the catalyst surface is composed of metal oxides, carbonates, and hydroxyl functionalities, which may contribute to its catalytic activity.

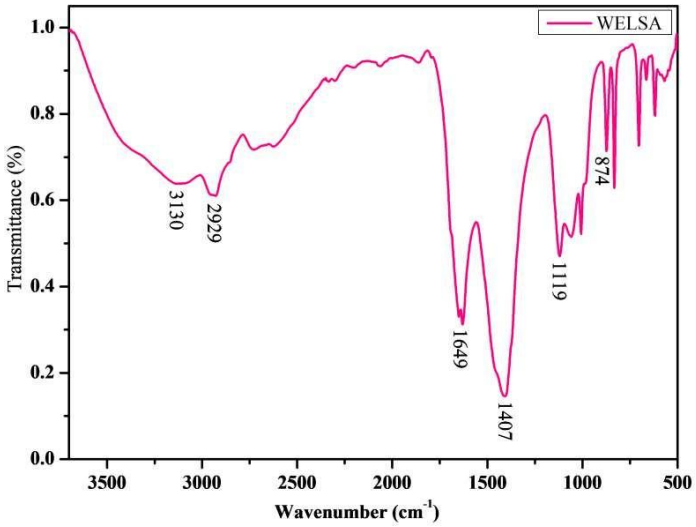

Fig. 3 FTIR spectrum of the *L. speciosa* fruit shells ash (WELSA).

The XRD pattern of the WELSA catalyst (**Fig. 4**) confirms the presence of crystalline metal oxides

and carbonate phases. The intense diffraction peaks at 2θ = 30.02° and 31.28° are assigned to K_2O and K_2CO_3, respectively. The characteristic peaks at 2θ = 32.30°, 34.04°, and 40.64° correspond to CaO (JCPDS: 002-1088) and $CaCO_3$ (JCPDS: 05-0586) phases, and the peak observed at 2θ = 42.94° is attributed to MgO, while the reflections at 2θ = 25.40° and 49.54° confirm the presence of SiO_2. Additionally, the peak at 2θ = 24.18° corresponds to Fe_2O_3. These Diffraction results collectively validate that the catalyst is composed of mixed oxides and carbonates, which are likely to contribute to its catalytic performance.

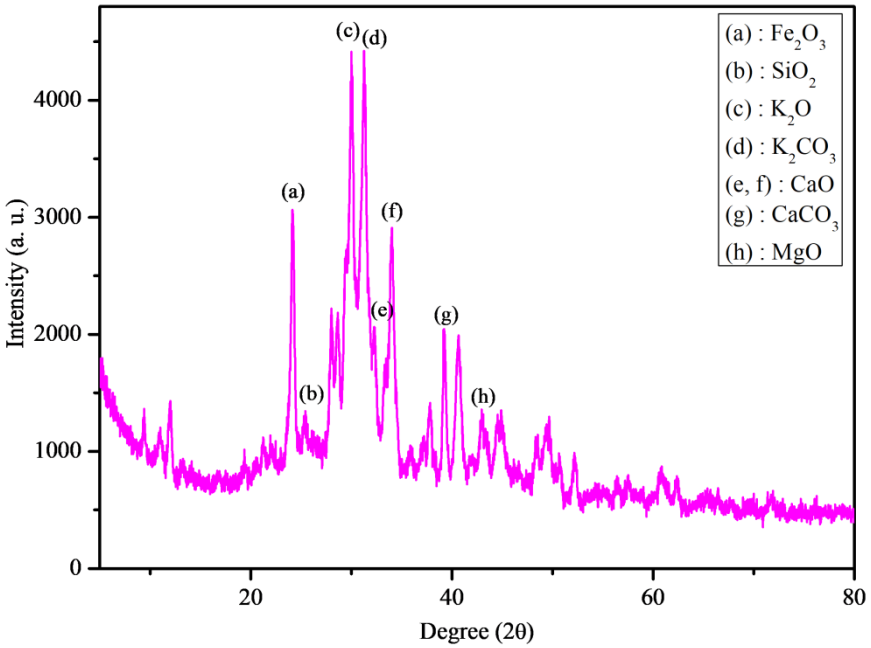

Fig. 4 XRD Pattern of the *L. speciosa* fruit shells ash (WELSA).

Scanning electron microscopy (SEM) was employed to examine the surface morphology and structural features of the catalyst, as shown in **Fig. 5**. The SEM micrographs reveal that the WELSA catalyst exhibit an irregular, porous framework with interconnected cavities and relatively smooth edges. The particles appear agglomerated and display a distinct flower-like morphology. Such a highly porous and textured surface is advantageous, as it provides an increased surface area and a higher density of active sites, which may enhance catalytic efficiency.

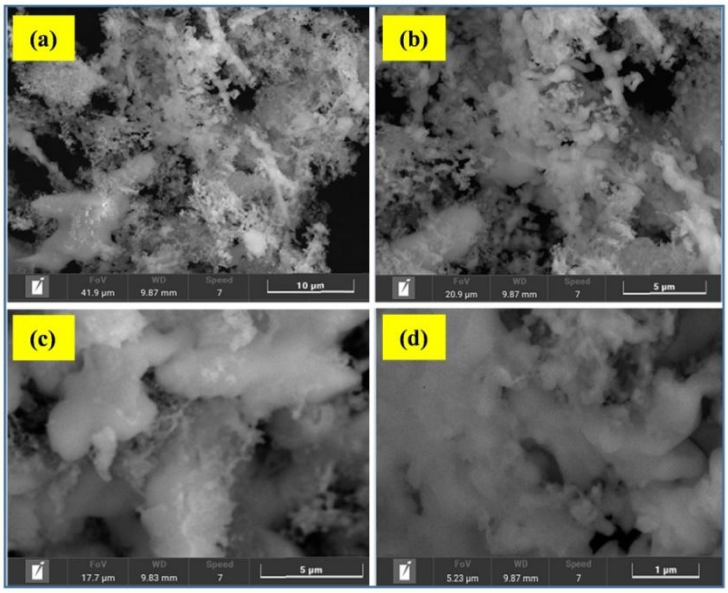

Fig. 5 SEM images **(5a-d)** of the *L. speciosa* fruit shells ash.

The elemental composition of WELSA catalyst was determined by Energy-dispersive X-ray (EDX) analysis, and the results are presented in **Fig. 6**. The EDX spectrum confirms the presence of Ca, Mg, K, Cu, Fe, C, and O and in the catalyst matrix, potassium identified as the most abundant element (Fig. 6). The dominance of K along with other metal constituents supports the mineral-rich and alkaline nature of the catalyst. These elements, particularly alkali and alkaline earth metals, are known to contribute the surface basicity and generation of active sites, which may play a key role in promoting its catalytic activity.

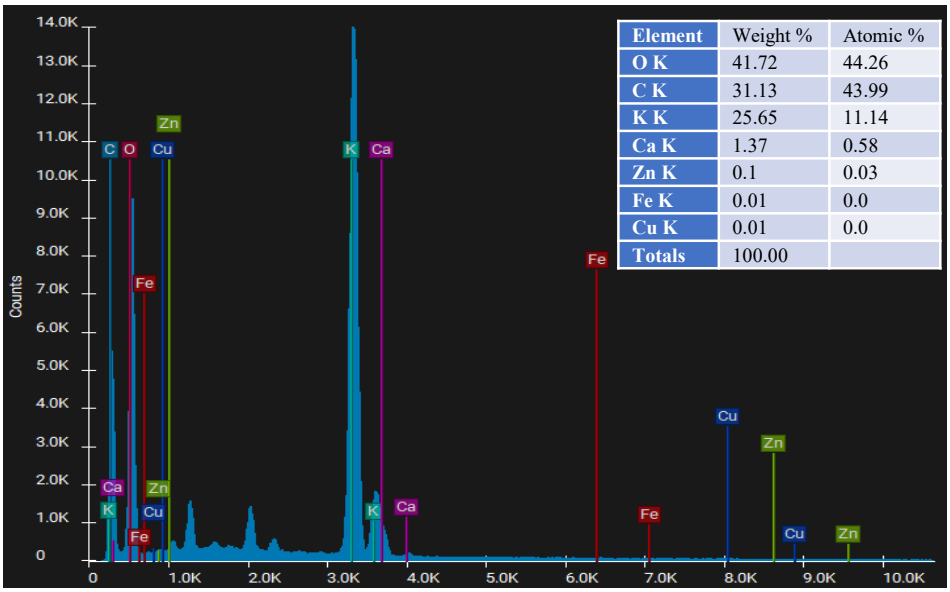

Fig. 6 EDX analysis of the *L. speciosa* fruit shells ash.

TGA-DTA was employed to investigate the thermal behavior of the WELSA catalyst, as shown in **Fig. 7**. The TGA profile of the WELSA catalyst exhibits three distinct weight-loss stages. The initial weight loss event observed below 150 °C in TGA and heat absorbed shown by deep endothermic peak in DTA corresponds to the evaporation of moisture and volatile components from the *L. speciosa* fruit shell ash. The

second significant weight-loss stage, occurring between 350–500 °C in TGA and broad exothermic event in DTA at 550 °C, is attributed to the decomposition of organic moieties. Furthermore, a third decomposition stage is observed above 650 °C, leaving behind a residue primarily composed of metal oxides such as CaO, MgO, Fe_2O_3, and SiO_2. The high thermal stability observed above 700 °C confirms the predominantly inorganic nature of the ash and highlights its potential as a thermally robust catalytic material.

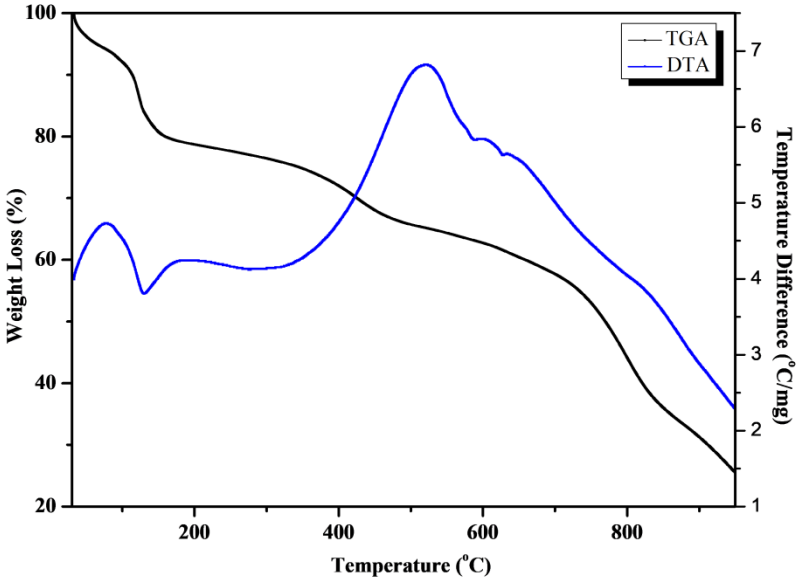

Fig. 7 TGA-DTA analysis of the *L. speciosa* fruit shells ash (WELSA).

3.2 Optimization of reaction conditions:

To establish the optimum reaction conditions for the synthesis of 2-amino-4*H*-benzochromene (**4a**), the reaction between benzaldehyde (1 mmol), malononitrile (1 mmol), and 1-naphthol (1 mmol) was selected as a model reaction system and carried out under various conditions using WELSA catalyst (Table 1). Initially, the model reaction was performed in the absence of the catalyst at room temperature and at 80 °C under solvent-free conditions (Table 1, entries 1–2); however, no improvement was observed even after a prolonged reaction time. Moreover, only trace amounts of product **4a** were obtained in aqueous and ethanolic media under the same conditions (Table 1, entries 3–4). Upon the addition of 1.0 mL of WELSA catalyst, the reaction proceeded under solvent-free conditions, highlighting its essential catalytic role (Table 1, entries 5–6). Subsequently, a series of experiments were conducted by varying the catalyst loading (1–3 mL) in aqueous and ethanolic media at room temperature (Table 1, entries 7–11). Increasing the catalyst volume led to complete conversion, affording the desired benzochromene in quantitative yield within 30 minutes, particularly in ethanol. Further increasing the catalyst amount to 4.0 mL did not significantly improve the yield or reduce the reaction time (entry 12). Notably, the use of 3.0 mL of WELSA in ethanol resulted in a 95 % yield within 30 min at room temperature (entry 11). In contrast, other solvents were less effective and resulted in lower yields (entries 13–16). Finally, based on the obtained results, 3.0 mL of WELSA catalyst in ethanol was selected as the optimal and green reaction condition, enabling rapid and efficient tandem Knoevenagel/Michael cyclization for the synthesis of **4a**.

Table 1 Optimization of reaction condition for synthesis of **4a**[a]

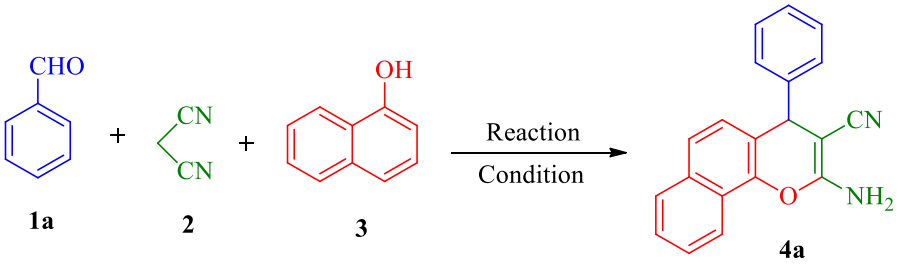

Entry	WELSA (mL)	Solvent	Temp. (ºC)	Time (min)	Yield (%)
1	-	-	r. t.	180	NR
2	-	-	80 ºC	180	NR
3	-	Water	80 ºC	180	Trace
4	-	Ethanol	80 ºC	180	Trace
5	1.0	-	r. t.	180	32
6	1.0	-	80 ºC	180	38
7	1.0	Water	r. t.	120	43
8	2.0	Water	r. t.	120	57
9	1.0	Ethanol	r. t.	120	65
10	2.0	Ethanol	r. t.	65	78
11	**3.0**	**Ethanol**	**r. t.**	**30**	**95**
12	4.0	Ethanol	r. t.	30	93
13	3.0	MeOH	r. t.	45	74
14	3.0	MeCN	r. t.	120	36
15	3.0	$CHCl_3$	r. t.	120	Trace
16	3.0	THF	r. t.	180	Trace

[a]Reaction conditions: benzaldehyde (1 mmol), Malononitrile (1 mmol) and 1-naphthol (1 mmol), WELSA catalyst, solvent (3 mL), room temperature. [b]Isolated yield.

In order to assess the applicability of the present protocol, a series of 2-amino-4*H*-benzochromene derivatives (**4a–r**) were synthesized under the optimized reaction conditions, and the results are summarized in **Table 2**. Both aromatic and heteroaromatic aldehydes bearing electron-withdrawing and electron-donating groups at different positions afforded the desired products (**4a–r**) in good to excellent yields (85–95%). The products were easily isolated from the reaction mixture and purified by recrystallization from ethanol. The synthesized 4*H*-benzochromene derivatives were further characterized by FT-IR, ^{1}H and ^{13}C NMR spectroscopy, mass spectrometry, and elemental analysis.

Table 2 Synthesis of 2-amino-4*H*-benzochromenes (**4a–r**) using WELSA catalyst.

Sr. No.	Aldehyde	α/β- naphthol	Product	Time (min)	Yield (%)
1	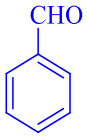	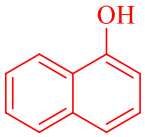	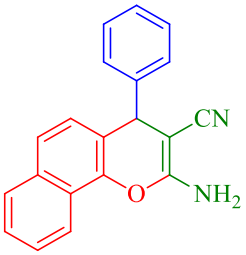 **4a**	30	95
2	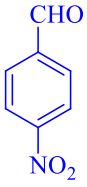	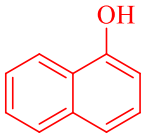	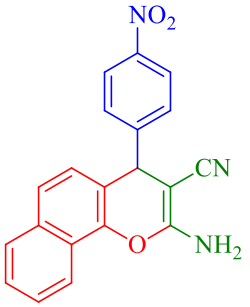 **4b**	25	85
3	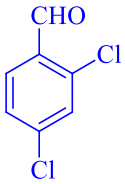	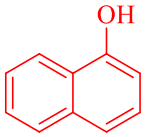	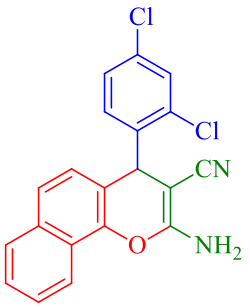 **4c**	35	88
4	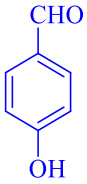	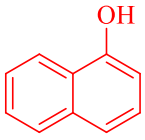	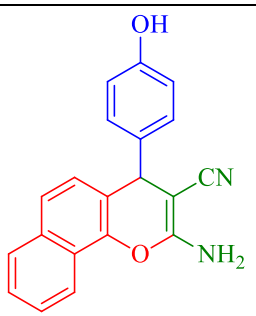 **4d**	30	86
5	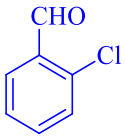	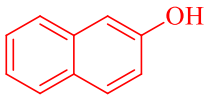	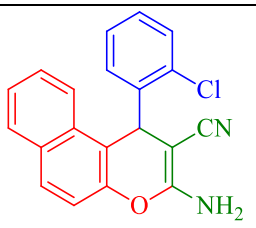	25	85

			4e		
6	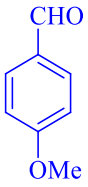	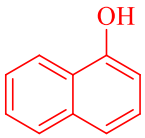	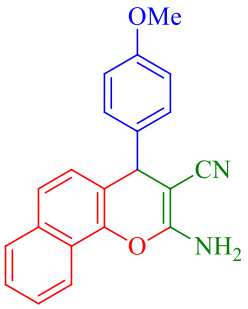 **4f**	20	87
7	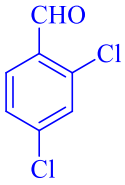	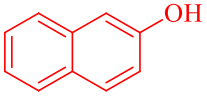	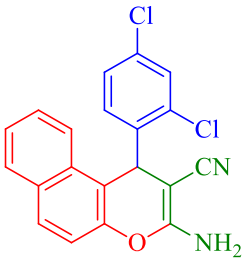 **4g**	30	86
8	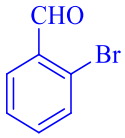	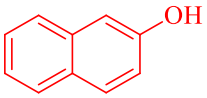	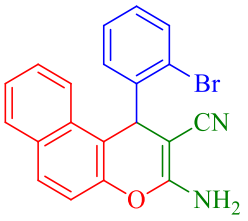 **4h**	20	86
9	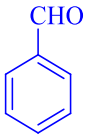	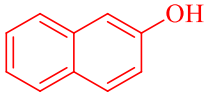	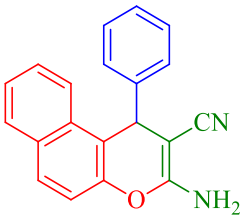 **4i**	30	94
10	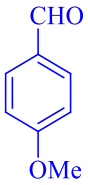	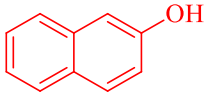	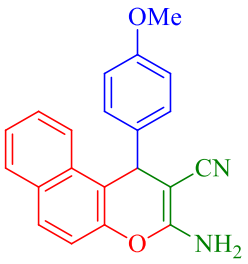 **4j**	25	94

11	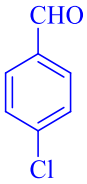	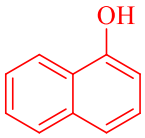	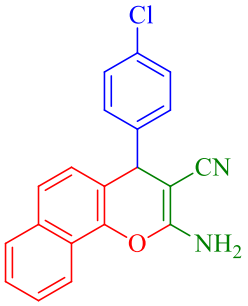 **4k**	20	90
12	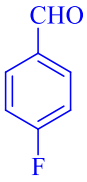	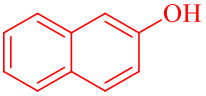	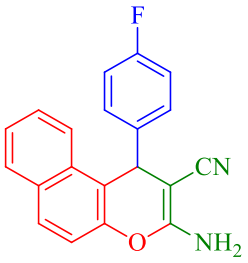 **4l**	30	84
13	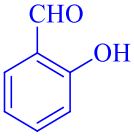	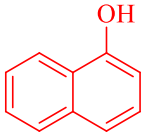	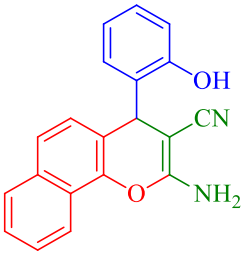 **4m**	35	82
14	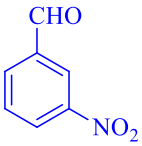	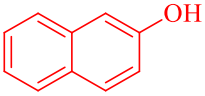	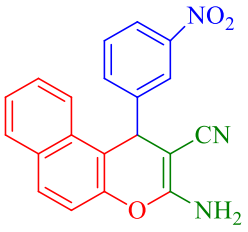 **4n**	40	85
15	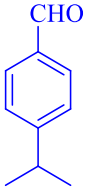	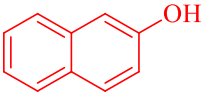	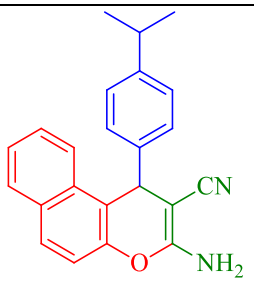 **4o**	30	82

16	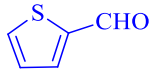	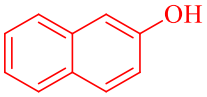	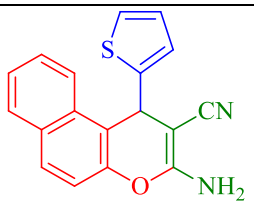 **4p**	40	86
17	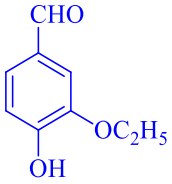	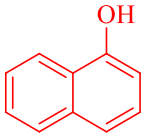	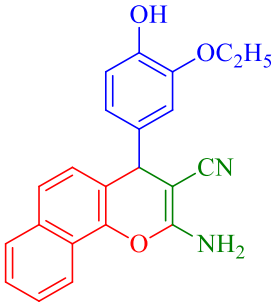 **4q**	35	84
18	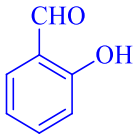	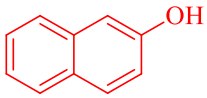	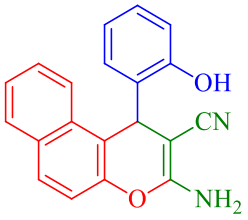 **4r**	30	86

[a]Reaction conditions: aldehydes (1 mmol), malononitrile (1mmol) and naphthols (1 mmol), WELSA catalyst (3 mL), ethanol (3 mL), RT. [b]Isolated yield.

3.3 Proposed reaction mechanism

On the basis of the obtained results and previous literature reports, a plausible mechanism for the synthesis of 2-amino-4*H*-benzochromene is depicted in **scheme 2**. Initially, a Knoevenagel adduct is generated through the condensation of benzaldehyde (**1a**) with malononitrile (**2**). The potassium ions present in WELSA activate the aldehyde, facilitating the nucleophilic attack of malononitrile to form intermediate (**I**). Subsequently, 1-naphthol undergoes nucleophilic attack on intermediate (**I**) via Michael addition, followed by intramolecular cyclization and proton transfer, ultimately affording the desired 2-amino-4*H*-benzochromene derivative (**4a**) [27].

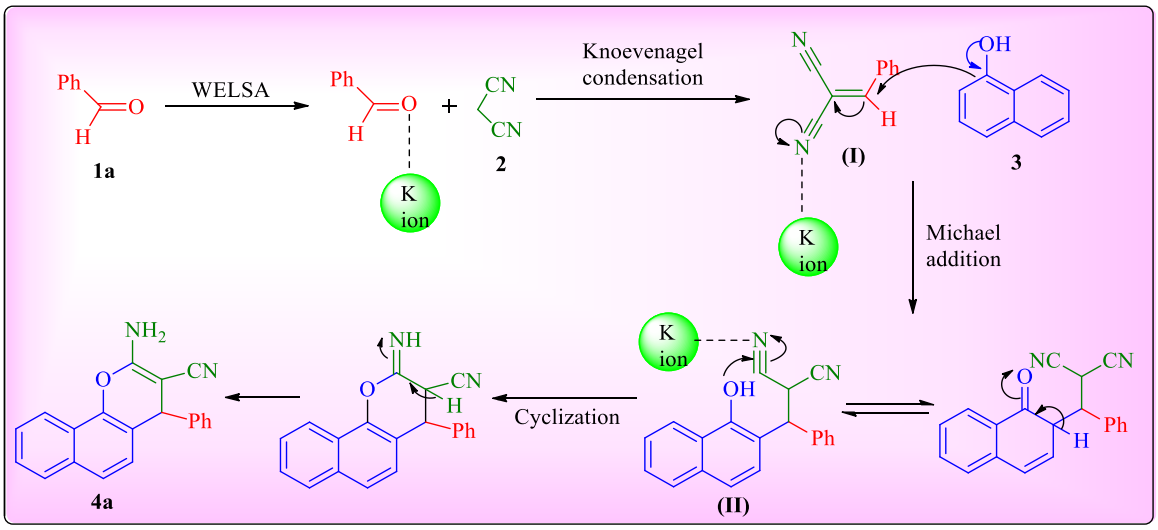

Scheme 2 Proposed reaction mechanism for the synthesis of 2-amino-4*H*-benzochromene (**4a**)

3.4 Reusability of catalyst

The recyclability and reusability of the WELSA catalyst for the synthesis of 2-amino-4*H*-benzochromene (**4a**) were evaluated over successive cycles under the optimized reaction conditions. After each reaction cycle, the product was separated by solvent extraction using ethyl acetate and further purified by recrystallization from hot ethanol. Meanwhile, the remaining aqueous layer containing the WELSA catalyst was vacuum-dried and subsequently reused for the next reaction cycle. It was observed that the catalyst retained excellent activity, affording isolated yields of 95 %, 92 %, 90 %, 88 %, and 86 % over five consecutive runs. The slight reduction in the yield can be attributed to the minimal catalyst loss during the isolation process and the deactivation of the catalyst. In general, the catalyst was stable and recyclable, emphasizing its potential as a sustainable catalyst in the synthesis of **4a** (**Fig. 8**).

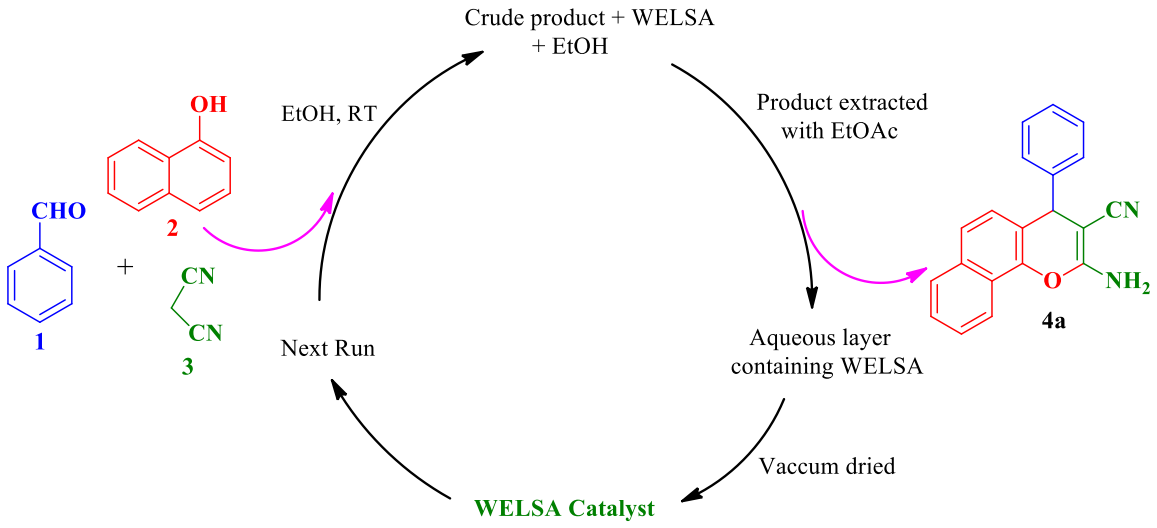

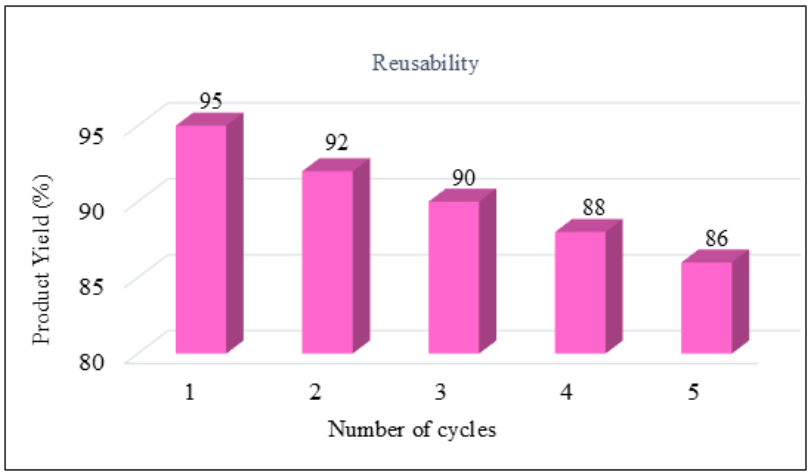

Fig. 8 Reusability of WELSA catalyst under optimized reaction conditions.

The results obtained in the present protocol have been compared with those available from other catalytic systems [28-35] and are presented in **Table 3**. Among these reported works, several catalysts afforded good yields of **4a**; however, they differed significantly in terms of reaction time and product yield. The use of ionic liquid and microwave-assisted systems demonstrated a noticeable effect; however same improvement was noticed using mineral base catalysts but generally required harsh reaction conditions. On the other hand, Biogenic catalysts operated under milder and greener reaction conditions. Notably, WELSA catalyst exhibited remarkable efficiency and stability offering 95 % product yield at room temperature within just 30 min., highlighting its potential as an efficient and sustainable catalytic system.

Table 3 Comparative evaluation of catalytic activity for the synthesis of **4a**.

Entry	Catalyst	Reaction conditions	Time (min.)	Yield (%) [Ref.]
1	$(NH_4)_2HPO_4$	EtOH:H_2O (1:1 v/v)	180	93 [28]
2	*p*-TSA	CH_3CN, Reflux	240	91 [29]
3	WEALA	RT	30	92 [30]
4	NH_4OAc	MW irradiation	4-5	85 [31]
5	CBS	RT	20	93 [32]
6	BFE	EtOH:H_2O (1:1 v/v)/RT	30	94 [33]
7	WEB	MW	2.5	79 [34]
8	WELFSA	M.W	2-8	90 [35]
9	**WELSA**	**EtOH/RT**	**30**	**95 [This work]**

4 Conclusion

The present investigation focused on the development of a novel catalytic system derived from the biowaste fruit shell ash of the plant *Lagerstroemia speciosa*. The resulting basic catalyst efficiently promoted the three-component synthesis of bioactive benzochromene derivatives in ethanol at room temperature without

the use of any external base catalyst. The key advantages of this protocol include the utilization of a natural, low-cost, and renewable feedstock, the use of a non-corrosive and reusable catalyst, high product yields under mild reaction conditions, a simple operational procedure, and good compliance with green chemistry principles. In addition, the recyclability of the WELSA catalyst was examined over several reaction cycles. The catalyst exhibited consistent performance over five consecutive cycles without any significant loss of catalytic activity. Overall, the present catalytic system provides a promising and sustainable alternative to conventional supported metal catalysts.

Abbreviations

FT-IR	Fourier Transform Infrared (FTIR) spectroscopy
XRD	X-ray Diffraction
EDX	Energy-dispersive X-ray analysis
SEM	Scanning electron microscopy
TGA	Thermogravimetric Analysis
DTA	Differential Thermal Analysis.
MCRs	Multicomponent reaction
TLC	Thin layer chromatography
DMSO	Dimethyl sulfoxide
JCPDS	Joint Committee on Powder Diffraction Standards
THF	Tetrahydrofuran
p-TSA	p-Toluenesulfonic Acid
WEALA	Water extract of Agave Americana leaf ash
CBS	Calcined snail shell
BFE	Bael fruit extract
WEB	Water extract of banana peel ash
WELFSA	Water extract of Lemon fruit shell ash
WELSA	Water extract of L. Speciosa fruit shell ash

Supporting Information

Spectral data (IR, ^{1}H and ^{13}C NMR, and Mass) of the representative compounds are provided in the supporting information file.

Acknowledgement

Authors are thankful to Punyashlok Ahilyadevi Holkar University, Solapur, CSIR-Indian of chemical Technology Tarnaka, Hyderabad and Central Facility Centre (CFC) Shivaji University, Kolhapur for providing necessary characterization facilities.

Funding Declaration

This research did not receive any specific grant from funding agencies in the public, commercial, or not-for-profit sectors.

Conflict of Interest

The authors declare that they have no known competing financial interests or personal relationships that could have appeared to influence the work reported in this paper.

References:

1. Sah MK, Ettarhouni ZO, Pathak R, Gawad J, Bonde C, Arya SP, Bhattarai A (2025) Green chemistry: strategies and sustainable approaches for bridging UN SDGS. Chemistry Select. https://doi.org/10.1002/slct.202500847
2. Garg MC, Kumari S, Nguyen, MK (2026) The role of green chemistry in the transformation of agro-industrial wastes for health and environment: a review. Biodegradation. https://doi.org/10.1007/s10532-026-10304-y
3. Bennett JA, Wilson K, Lee A (2016) Catalytic applications of waste derived materials. J. Mater. Chem. A. https://doi.org/10.1039/c5ta09613h
4. Patil UP, Patil RC, Patil SS (2019) An eco-friendly catalytic system for one-pot multicomponent synthesis of diverse and densely functionalized pyranopyrazole and benzochromene derivatives. J. Heterocyclic Chem. https://doi.org/10.1002/jhet.3564
5. Patil UP, Patil SU (2024) Natural base catalysis in the sustainable synthesis of functionalized 2-amino-4H-chromenes. Iran. J. Catal. 10.57647/j.ijc.2024.1402.16
6. Patil UP, Patil RC, Patil SS (2021) Biowaste-derived heterogeneous catalyst for the one-pot multicomponent synthesis of diverse and densely functionalized 2-amino-4*H*-chromenes. Org. Prep. Proced. Int, https://doi.org/10.1080/00304948.2020.1871309
7. Patil UP, Patil RC, Patil SS (2020) Waste mussel shell as a highly efficient heterogeneous catalyst for the synthesis of polyfunctionalized 4*H*-pyrans in aqueous media. Reac Kinet Mech Cat. https://doi.org/10.1007/s11144-020-01743-6
8. ALI EA (2019) Medical value of lagerstroemia speciosa: an updated review. Int. J. Curr. Pharm. Res. https://doi.org/10.22159/ijcpr.2019v11i5.35708
9. Lai KH, Darah I, Wong CT, Lim SH (2015) In vitro antibacterialactivity and cytotoxicity of Lagerstroemia speciosa bark extract. Indian journal of pharmaceutical science. 10.4172/pharmaceutical-sciences.1000113
10. Yanlong Gu (2012) Multicomponent reactions in unconventional solvents: state of the art. Green Chem. https://doi.org/10.1039/c2gc35635j
11. a) Pertwee RG (2002) Cannabinoids and multiple sclerosis. Pharmacol. Ther. https://doi.org/10.1016/S0163-7258(02)00255-3; b) Massaga C, Paul L, Kwiyukwa LP, Vianney J, Chacha M, Raymond J (2025) Computational analysis of Urolithin A as a potential compound for anti-inflammatory, antioxidant, and neurodegenerative pathways. Free Radic. Biol. Med. https://doi.org/10.1016/j.freeradbiomed.2024.12.003; c) Gewali MB, Banskota TY, Ali AH, Saiki I, Dong H, Kadota S (1999) Epicalyxin F and calyxin I: two novel antiproliferative diarylheptanoids from the seeds of alpinia blepharocalyx. Org. let. https://doi.org/10.1021/ol990260p; d) Cadelis MM, Bourguet-Kondracki ML, Dubois J, Valentin A, Barker D, Copp BR (2016) Discovery and preliminary structure–activity relationship studies on tecomaquinone I and tectol as novel farnesyltransferase and plasmodial inhibitors. Bioorg. Med. Chem. 10.1016/j.bmc.2016.05.024
12. Kamdar NR, Haveliwala DD, Mistry PT, Patel SK (2011) Synthesis and evaluation of in-vitro antitubercular activity and antimicrobial activity of some novel 4*H*-chromeno[2,3-*d*] pyrimidine via 2-

amino-4-phenyl-4H-chromene-3-carbonitriles. Med Chem Res. https://doi.org/10.1007/s00044-010-9399-x

13. Sivaguru P, Sandhiya R, Adhiyaman M, Lalitha A (2016) Synthesis and antioxidant properties of novel 2H-chromene-3-carboxylate and 3-acetyl-2H-chromene derivatives. Tetrahedron Lett. 10.1016/j.tetlet.2016.04.097
14. Ezzatzadeh,E., Hossaini,Z. (2020) Four-component green synthesis of benzochromene derivatives using nano-KF/clinoptilolite as basic catalyst: study of antioxidant activity. Mol Divers. https://doi.org/10.1007/s11030-019-09935-6.
15. Kamdar NR, Haveliwala DD, Mistry PT, Patel SK (2010) Design, synthesis and in vitro evaluation of antitubercular and antimicrobial activity of some novel pyranopyrimidines. Eur. J. Med. Chem. 10.1016/j.ejmech.2010.08.014.
16. Jesumoroti OJ, Mnkandhla D, Isaacs M, Hoppe HC, Klein R. (2019) Evaluation of novel N′-(3-hydroxybenzoyl)-2-oxo-2H-chromene-3-carbohydrazide derivatives as potential HIV-1 integrase inhibitors. Med. Chem. Commun. https://doi.org/10.1039/c8md00328a

17 Maddahi M, Asghari S, Pasha G (2023) A facile one-pot green synthesis of novel 2-amino -4H-chromene: antibacterial and antioxidant evaluation. Res. Chem. Intermed. 10.1007/s11164-022-04893-5

18 Yanyang He, Rong Hu,Tong R, Shi J, Zhang M (2014) K_2CO_3-Mediated Synthesis of Functionalised 4-Substituted-2-amino-3-cyano-4*H*-chromenes via Michael-Cyclization Reactions. Mol. https://doi.org/10.3390/molecules191219253

19 Raj V, Lee J (2020) 2*H*/4*H*-Chromenes—A versatile biologically attractive scaffold. Front Chem. 10.3389/fchem.2020.00623

20 EI-Agrody A, Fouda A, Khattab E(2013) Synthesis, antitumor activity of 2-amino-4H-benzo[h] chromene derivatives, and structure-activity relationships of the 3-and 4-positions.Med. chem. res. 10.1007/s00044-013-0602-8

21 Dgachi Y, Bautista-Aguilera O, Benchekroun M (2016) Synthesis and biological evaluation of benzochromenopyrimidinones as cholinesterase inhibitors and potent antioxidant, non-hepatotoxic agents for Alzheimer's disease. Mol. https://doi.org/10.3390/molecules21050634

22. Abbaszadeh-Mahmoudi E, Shirzaei F, Shaterian H (2025) Preparation of new benzochromene derivatives using triethylamine, 2-hydroxyethylammonium formate, and Fe3O4@SiO2@[O-(CH2)2-NH2][HCO2H] as catalysts. Res. Chem. Intermed. 10.1007/s11164-025-05698-y

23 Patil UP, Patil RC, Patil SS (2019) An eco-friendly catalytic system for one-pot multicomponent synthesis of diverse and densely functionalized pyranopyrazole and benzochromene derivatives. J. Heterocyclic Chem. https://doi.org/10.1002/jhet.3564

24. Ghabdian K, Motavalizadehkakhky A, Zhiani R, Allahresani A (2024) Cu(II) salen complex grafted onto KCC-1 as a convenient multifunctional heterogeneous catalyst for the preparation of 4*H*-benzochromenes. Res. Chem. Intermed. 10.1007/s11164-024-05311-8

25. Tazari M, Kiyani H (2019) Expeditious synthesis of 2-Amino-4*H*-chromeneand 2-amino-4*H*-Pyran-3-carboxylates promoted by sodium malonate. Curr. Org. Synth. 10.2174/1570179416666190415105818

26. Rezvaneh R, Mohammad AK, Daryoush Z (2022) Wood ash biocatalyst as a novel green catalyst and its application for the synthesis of benzochromene derivatives**.** Sci Rep.

https://doi.org/10.1038/s41598-022-05133-x

27. Kerru N, Gummidi L, Bhaskaruni S, Maddila S (2020) One-pot green synthesis of novel 5,10-dihydro-1H-pyrazolo[1,2-b]phthalazine derivatives with eco-friendly biodegradable eggshell powder as efficacious catalyst. Res. Chem. intermed. 10.1007/s11164-020-04135-6
28. Kerru N, Gummidi L, Bhaskaruni S, Maddila S, Jonnalagadda S (2020) A review of recent advances in the green synthesis of azole-and pyran-based fused heterocycles using MCRs and sustainable catalysts. Res. Chem. Intermed. 10.2147/138527282499920102020462O
29. Baghernejad B, Heravi M, Oskooie H (2009) A Novel and Efficient Catalyst to One-Pot Synthesis of 2-Amino4H-chromenes by p-Toluenesulfonic Acid J. Korean Chem. Soc. 10.5012/jkcs.2009.53.6.631
30. Patil U, Patil R, Patil S (2019) An eco-friendly catalytic system for one-pot multicomponent synthesis of diverse and densely functionalized pyranopyrazole and benzochromene derivatives. J. Hetero. Chem. https://doi.org/10.1002/jhet.3564
31. Shah NK, Shah NM, Patel MP, Patel RG (2013) Synthesis of 2-amino-4H-chromene derivatives under microwave irradiation and their antimicrobial activity. J. Chem. Sci. https://doi.org/10.1007/s12039-013-0421-y
32. Patil UP, Patil SU (2024) Natural base catalysis in the sustainable synthesis of functionalized 2-amino-4H-chromenes. IJC. https://doi.org/10.57647/j.ijc.2024.1402.16
33. Shinde S, Damate S, Morbale S, Patil M, Patil S (2017) Aegle marmelos in heterocyclization: greener, highly efficient, one-pot three-component protocol for the synthesis of highly functionalized 4*H*-benzochromenes and 4*H*-chromenes. RSC Adv. 10.1039/C6RA28779D
34. Kantharaju K, Khatavi S (2018) A green method synthesis and antimicrobial activity of 2-amino-4*H*-chromene derivatives. Asian J. chem. https://doi.org/10.14233/ajchem.2018.21191
35. Kantharaju K, Khatavi S (2018) Microwave accelerated synthesis of 2-amino-4*H*-chromenes catalyzed by WELFSA: a green protocol. Chemistry Select. https://doi.org/10.1002/slct.201800096

Figure Title and Legend section

Figure 1 Glimpse of plant products bearing benzochromene moieties.

Figure 1 represents some naturally occurring bioactive benzochromenes, such as tetrahydrocannabinol [**A**], urolithin [**B**], epicalyxin F [**C**], and tectol [**D**], which exhibit multiple sclerosis, anti-inflammatory, anticancer, and antiplasmodial activities

Figure 2 Preparation of the WELSA catalyst

The stepwise preparation of the WELSA catalyst from dried *Lagerstroemia speciosa* fruit shells by thermal treatment.

Figure 3 FTIR spectrum of the *L. speciosa* fruit shells ash (WELSA).

The FTIR spectrum of the WELSA catalyst revealed the presence of metal oxides, carbonates, and hydroxyl groups on its surface, which are likely responsible for its catalytic activity.

Figure 4 XRD Pattern of the *L. speciosa* fruit shells ash (WELSA).

The XRD pattern of the WELSA catalyst confirms the presence of crystalline metal oxides and carbonate phases.

Figure 5 SEM images **(5a-d)** of the *L. speciosa* fruit shells ash.

The SEM images disclosed the agglomeration and flower-like morphology of WELSA catalyst. Such a highly porous and textured surface is advantageous, as it provides an increased surface area and a higher density of active sites, which may enhance catalytic efficiency.

Figure 6 EDX analysis of the *L. speciosa* fruit shells ash.

The EDX spectrum confirms the presence of Ca, Mg, K, Cu, Fe, C, and O and in the catalyst matrix. The dominance of K along with other metal constituents supports the mineral-rich and alkaline nature of the catalyst.

Figure 7 TGA-DTA analysis of the *L. speciosa* fruit shells ash (WELSA).

The TGA–DTA analysis revealed that the WELSA catalyst exhibits high thermal stability above 700 °C, confirming the predominantly inorganic nature of the ash and highlighting its potential as a thermally robust catalytic material.

Figure 8 Reusability of WELSA catalyst under optimized reaction conditions.

The reusability study demonstrated that the WELSA catalyst retained excellent catalytic activity for up to five consecutive reaction cycles.

Supplementary Files

This is a list of supplementary files associated with this preprint. Click to download.

- SupplementaryInformation.docx